

Molecular Dynamics Study of Aqueous NaCl Solution: Flush Crystallization Caused by Solution Phase Change

K. Kobayashi · Y. Liang · T. Matsuoka

Received: date / Accepted: date

Abstract Solutions at sub- or supercritical conditions receive much attention due to its significance in geology and applications in industrial process. Armellini and Tester showed the experimental results where sodium chloride solution was rapidly mixed with sub- or supercritical water. The morphology difference was observed in the experiment at different pressures. Sodium chloride crystal, which was formed at lower pressure, 200bar, showed porous morphology. In contrast, the crystal formed at higher pressure, 250bar, was amorphous like in shape. The mechanism was explained that the porous crystal came from rapid crystallization without forming vapor-liquid coexistence phase. However, due to short time scale, experimental observation of the underlining mechanism is difficult. Here we conducted micro second time scale molecular dynamics with interfacial system. The correlation between number density of ions and water was proposed to parametrize the solution phase. The correlation and the two dimensional number densities provided us the atomic insight of the flush crystallization, where the vapor-liquid coexistence phase was found at high pressure. Finally, we support the mechanism for the morphology difference from theoretical point of view.

Keywords Supercritical · Crystallization · Molecular Dynamics

K. Kobayashi
Environment and Resource System Engineering Lab., Kyoto Univ.
Tel.: +81-75-383-3206
Fax: +81-75-383-3203
E-mail: kobayashi.kazuya.44n@st.kyoto-u.ac.jp

Y. Liang
Environment and Resource System Engineering Lab., Kyoto Univ.
Tel.: +81-75-383-3205
Fax: +81-75-383-3203
E-mail: liang.yunfeng.5x@kyoto-u.ac.jp

T. Matsuoka
Environment and Resource System Engineering Lab., Kyoto Univ.
Tel.: +81-75-383-3201
Fax: +81-75-383-3203
E-mail: matsuoka.toshifumi.7x@kyoto-u.ac.jp

1 Introduction

Aqueous solutions are essential to life, biology, chemistry, and geology owing to their ubiquitousness in nature. The reason why crystallization under high pressure and high temperature condition receives much attention is due to extremely low salt solubility under such condition. At this condition, aqueous solutions can change its phase and the flush crystallization occurs[1,2]. From geological aspect, it indicates how the huge geological salt system formed[3] under high pressure and high temperature (e.g. around oceanic volcanoes in ocean ridges). It is supposed that solution phase change leads precipitations of salts, and an extremely low salinity vent fluid is actually found around the oceanic volcano[4]. For example, it was reported that the hydrothermal system at the Mid-Atlantic Ridge discharges the vent fluid above 407°C at around ~3000m water depth, where decreased salinity in the vent fluid was observed[5]. There are also several cites in deep sea where vent fluid condition locates near from the phase boundary [6–12]. In addition, such kind of condition can be found in a deep crust in the earth where subducting seawater interacts with extremely hot earth mantle[13]. Understanding of seawater at the extreme conditions are the key to reveal water and salts cycle in the deep sea. On the other hand, solutions at extreme conditions are also of importance for industrial Super Critical Water Oxidization(SCWO) process. The technology presents important environmental advantages for the treatment of industrial waste and sludges[14]. The salt due to extremely low solubility can clog the equipments of super critical oxidization process.

First visual observation has been conducted by Armellini, Tester, and Hong[1, 2]. They rapidly mixed sodium chloride solution with super critical water in order to observe the flush crystallization at different pressures. The results provided us the crystal morphology difference, which was explained by phase behavior of salt solution. Under higher pressure, 250bar, the solution formed vapor-liquid coexistence phase before crystallization, as a result, amorphous like crystal formed. In contrast under lower pressure, 200bar, porous crystal formed because the salt rapidly crystallized without forming vapor-liquid coexistence phase. However the kinetics of the mechanism is still unclear due to short time scale of the phenomenon. The motivation of our study is to reveal the kinetics of the flush crystallization with short time window by using molecular dynamics (MD). The technique can provide us the dynamics of salt formation with pico-second time window until micro-second time scale.

This paper is divided into four parts. In Sect.2, the simulation detail is provided. The results and discussion are in Sect.3. Finally, we will provide conclusion in Sect.4.

2 Methodology

GROMACS (ver. 4.5.4)[15] was used for calculation engine of MD. SPC/E water model[16,17] was used in this study. For sodium and chloride model, Joung and Cheatham ionic models[18] were used. The ionic models are compatible for SPC/E water and its calculated solubility value was reported as 7.27mol/kg at the ambient condition[19]. It is supposed that the model describes both ion-ion interaction and ion-water interaction well. The system includes 500 pairs of ion in solid phase and

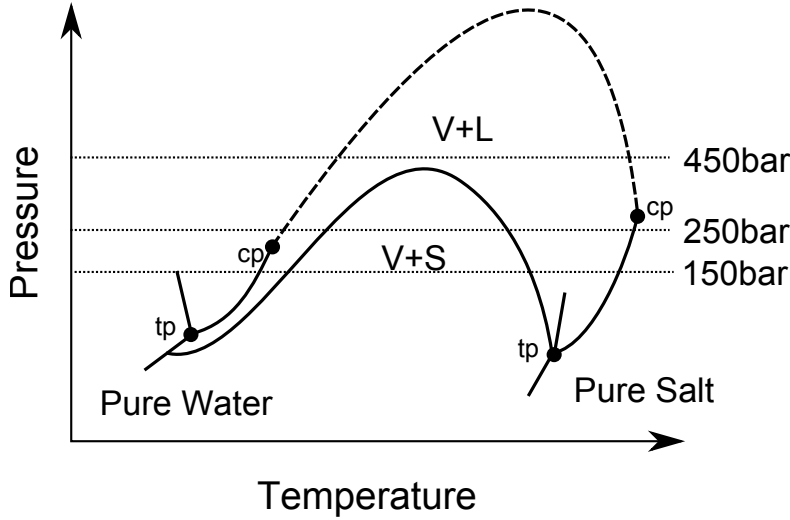


Fig. 1 Simulation pressures overlapping with schematic phase diagram of sodium chloride solution which was shown in Ref. [1].

solution phase has 2000 water molecules and 320 pairs of ion, where the solution is supersaturated even at ambient condition. Combining the solid and the solution, we constructed the interfacial simulation system.

The phase diagram of sodium chloride was shown by the several authors[20–23]. We thus chose the pressure point where the behavior of the sodium chloride solution is expected to change. The calculation pressures were chosen as 150bar, 250bar, and 450bar, where they are below the critical pressure of pure water, between the critical pressure of water and the critical pressure of vapor–solid region for sodium chloride solution system, and above the critical pressure of vapor–solid region, respectively[23](Fig.1). Since phase boundary of the simulation system has been unknown, we divided our calculation into two parts. The first was 50K temperature increment calculation starting from 600K, where the same configuration was selected for initial configuration. The system equilibration can be easily judged in the calculation because the concentration in the solution decreases dramatically when the system goes to the equilibrated state. In the calculation, if the dramatic volume change, which is defined as over 30% increment from the previous temperature, is observed, we switched the calculation to the second one. The second calculation is started with configuration which is 50K temperature before the temperature point of the dramatic volume change. The system at this temperature is run until the ionic concentration of the solution phase is converged at the last 150ns. The temperature is then increased 10K every 500ns calculation until the dramatic volume change is observed. We thus conducted maximum 1.2-2.7 μ s in the second run. It enables us to observe more realistic kinetics of the flush crystallization. All the calculations are executed with NPT ensemble, where the temperature is controlled by Nose-Hoover thermostat[24] and the pressure is controlled by Parinello-Rahmann barostat[25]. Snapshots were prepared by visual molecular dynamics (VMD) software[26].

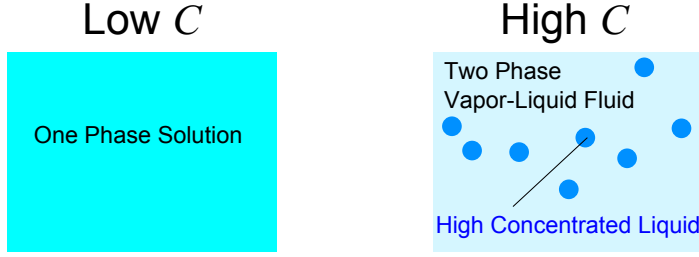


Fig. 2 Schematic diagram of liquid-vapor coexistence and the relationship with the C (correlation) value.

A key to observe the kinetics of the flush crystallization is the parametrization of solution states during the simulation. We propose that the correlation coefficient between the density of water and the density of ions can be used to evaluate the solution state in short time step. In one phase solution, ions and water are uniformly distributed. Therefore, there is less correlation between the two number density maps. However, if the fluid forms vapor-liquid coexistence phase, the high density contrast of ions and water will lead high correlation values (Fig.2). The mathematical definition follows:

$$C = \frac{\sum_i \left(n_i^{\text{NaCl}} - \overline{n^{\text{NaCl}}} \right) \left(n_i^{\text{Water}} - \overline{n^{\text{Water}}} \right)}{\sqrt{\sum_i \left(n_i^{\text{NaCl}} - \overline{n^{\text{NaCl}}} \right)^2} \sqrt{\sum_i \left(n_i^{\text{Water}} - \overline{n^{\text{Water}}} \right)^2}} \quad (1)$$

where n_i^A is the number density of component A in the grid i and $\overline{n^A}$ means the average of number density of the component in solution area. In this work we did not construct three dimensional number density grid because the system has homogeneity in x-y plane. y-z two dimensional number density with $1\text{\AA} \times 1\text{\AA}$ was thus chosen. The two dimensional number density was calculated from 100ps average with 100 frames. In order to evaluate only the solution area, the definition of the solution area was set. It was defined as the area where the initial crystal area and 2.0nm area from the initial crystal surface, except as otherwise provided, was excluded from whole of the system. The method can be applied for completely heterogeneous system by calculating three dimensional number density grid for another work.

3 Results and Discussion

3.1 150bar

As described in Sect.2, two kinds of simulation have been executed. One was starting with the same initial configuration with 50K temperature step. The other was 10K temperature increment every 500ns continuously in order to observe dynamic behavior of the flush crystallization. From the first calculation the dramatic volume change was observed at 700K calculation. It meant there was phase boundary between 650K and 700K in the system. We thus implemented the second calculation starting from the final configuration of the 650K calculation. The calculated correlation as the function of time was shown in Fig.3. The equilibration was observed around 400ns in the 650K calculation which reflected rapid crystallization in the system due to supersaturated nature in the initial configuration. In the period of 660K the correlation value was fluctuated but stable around 0.1. It can be interpreted that there is no vapor-liquid coexistence phase in the system, which was also confirmed by two dimensional number density maps (Fig.4). After the temperature was increased to 670K, dramatic change in the correlation which meant vaporization of the solution was observed. Interestingly, an isolated solid phase formed in the system after the high correlation condensed phase was found in very short time (Fig.5). And it reduced the correlation value at the end of the simulation. Both from the correlation and from the number density maps, it was suggested that the crystallization at 150bar occurred in very short time scale (~ 20 ns). Very short time scale in the crystallization encourages formation of the isolated crystal, which may reflect the porous crystal morphology observed in the experiment[2].

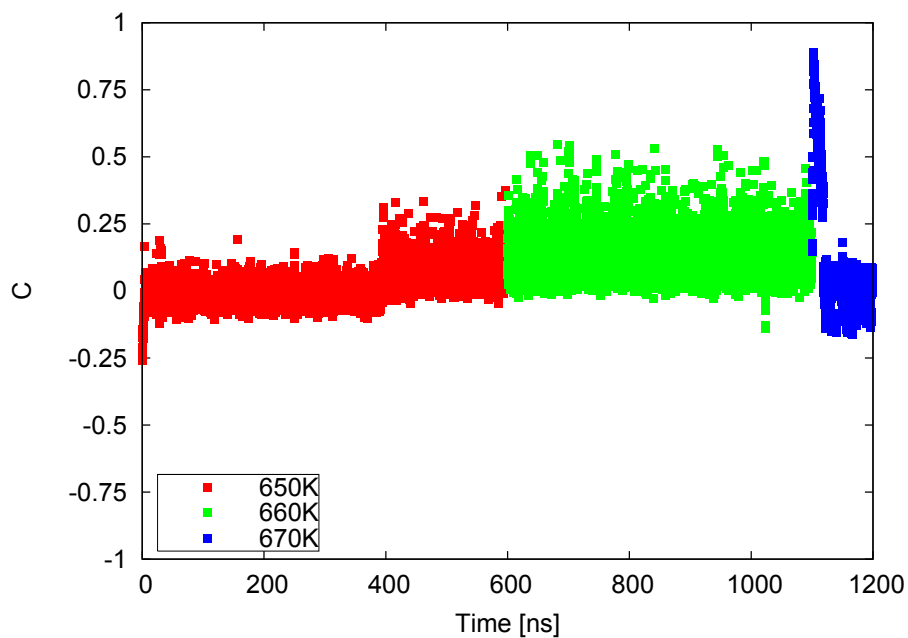


Fig. 3 Correlation coefficient with 10K increment every 500ns from 650K at 150bar.

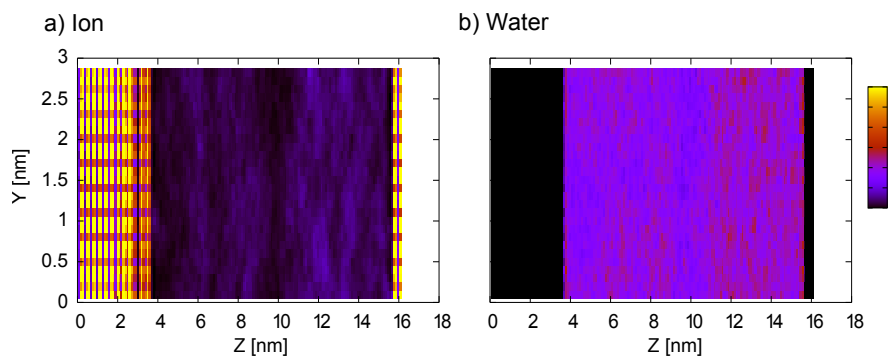


Fig. 4 Number density maps at the point of $t = 1000\text{ns}$, $T = 660\text{K}$, $C = 0.143$. Left and right figures show the number densities of ions and water, respectively.

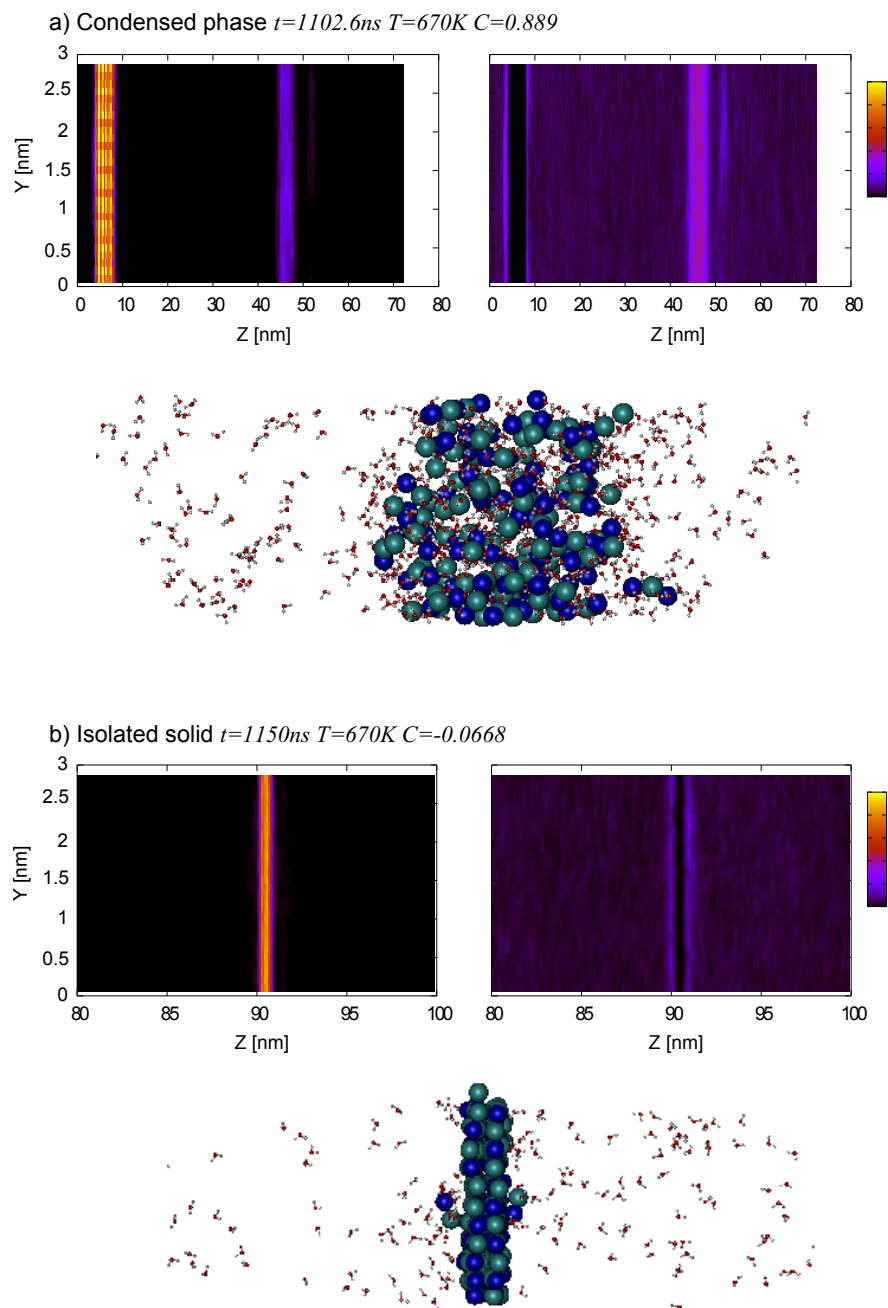


Fig. 5 Number density maps and snapshots of condensed phase and isolated solid. In (a) and (b), left and right figures show the number densities of ions and water, respectively.

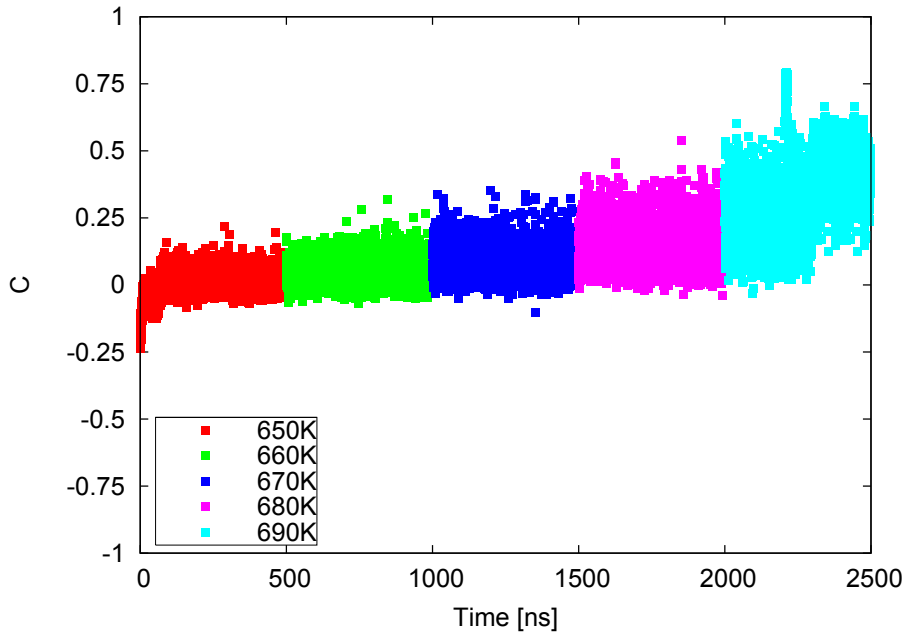


Fig. 6 Correlation coefficient with 10K increment every 500ns from 650K at 250bar.

3.2 250bar

In the 250bar case, the dramatic volume change was also found at 700K. We thus executed the 10K increment calculation toward 700K starting from the final configuration at 650K. The correlation result is shown in Fig.6, where the gradual increasing in the correlation was found. And the number density maps are also shown in Fig.7. The low density area of water and high density area of water which correlated with the number density of ions could be found. It was suggested that the existence of the high concentrated liquid phase and the low concentrated vapor phase in the solution area contributed to high correlation values during the simulation in contrast to the 150bar calculation. As the temperature was increased, the density contrast became significant. And after correlation peak around 2200ns at 690K, we finally observed vapor-solid phase from the number density maps as seen at 150bar. This observation is consistent with experiments where 250bar locates between the critical pressure of pure water and the critical pressure of the vapor-solid region. Since the crystallization during the simulation occurred with the liquid-vapor coexistence, the time for crystallization was longer than the case of the 150bar calculation. As a result, there was no isolated solid. The fact agrees with the proposed mechanism of the crystal morphology difference by Armellini, Tester, and Hong[2]. At the time, due to adsorbed water correlated with sodium chloride ion at the interface, correlation has not been decreased dramatically. This has been confirmed by changing the solution area definition, where the correlation values after the peak (~ 2200 ns) became almost zero ($\sim 10^{-2}$) when we increased the exclusion area to 4.0nm from the initial crystal.

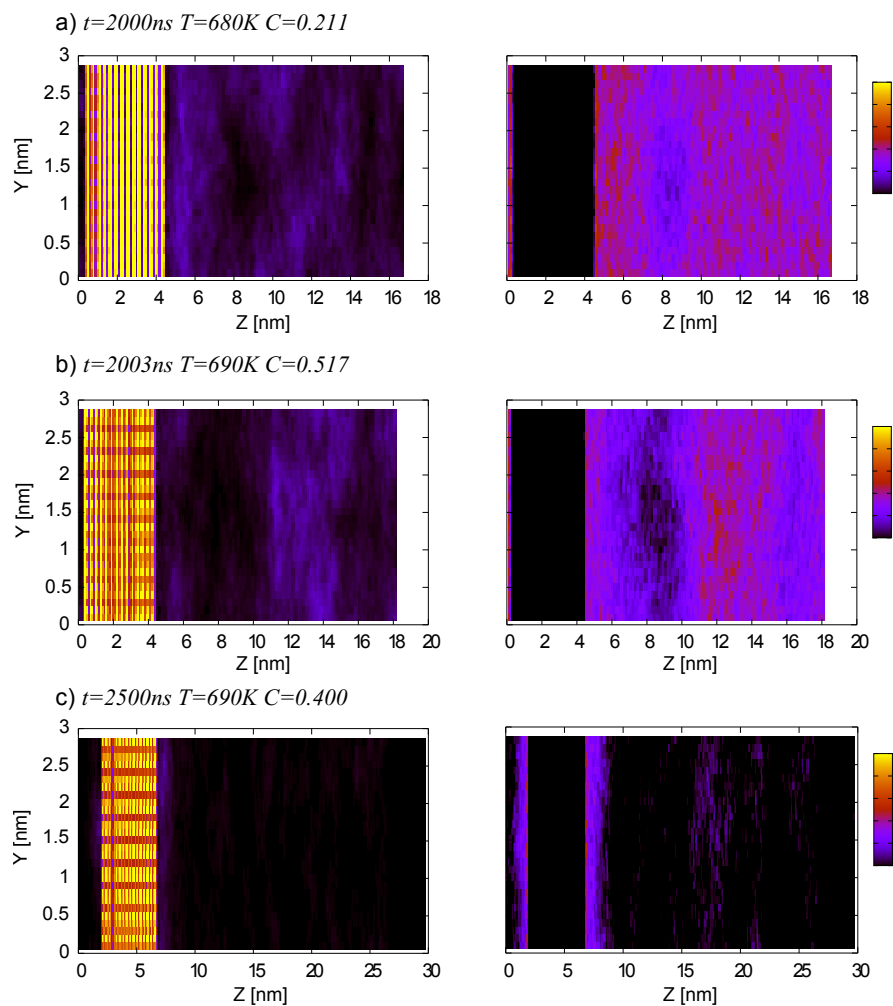


Fig. 7 Number density maps at 250bar. Left and right figures show the number densities of ions and water, respectively.

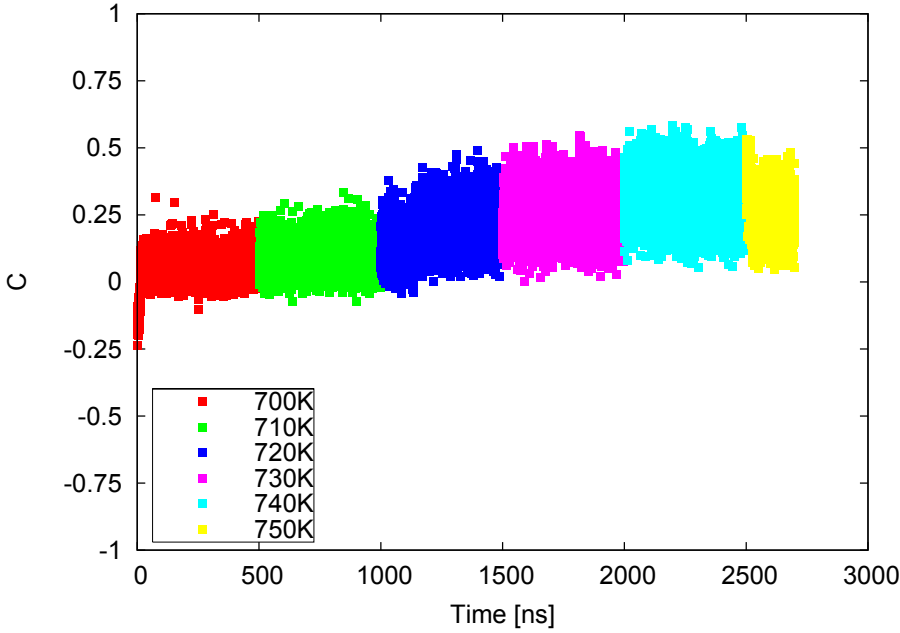


Fig. 8 Correlation coefficient with 10K increment every 500ns from 700K at 450bar.

3.3 450bar

Due to higher pressure, the dramatic volume change was found at higher temperature, 750K, than the previous two in the first calculation. We thus conducted the 10K temperature step calculation starting from the final configuration at 700K. The time evolution of the correlation was similar as the case of 250bar (Fig.8). It suggested the existence of the high concentrated liquid phase and the low concentrated vapor phase as seen in the 250bar calculation. However the correlation peak could not be observed in this case, while the total number of the sodium chloride pair continuously decreased within the vapor-liquid coexistence phase. The fact can be seen from the number density maps as shown in Fig.9. The number density maps from the last 100ps showed that there was still vapor-liquid coexistence, which agreed with the phase diagram of the sodium chloride solution.

3.4 Discussion

One of our intentions was the parametrization of the solution states. The correlation can work as the good indicator whether vapor-liquid coexistence phase is in the system or not. Because the expected correlation value will be high when the high concentration liquid phase and the low concentration vapor phase form (Fig.2). By the analysis, we could point when the phase change occurred, which helps us to observe the system state in detail. The mechanism of crystal morphology by Armellini, Tester, and Hong[2] was that vapor-liquid coexistence phase could form during the flush crystallization in the high pressure regime, where the

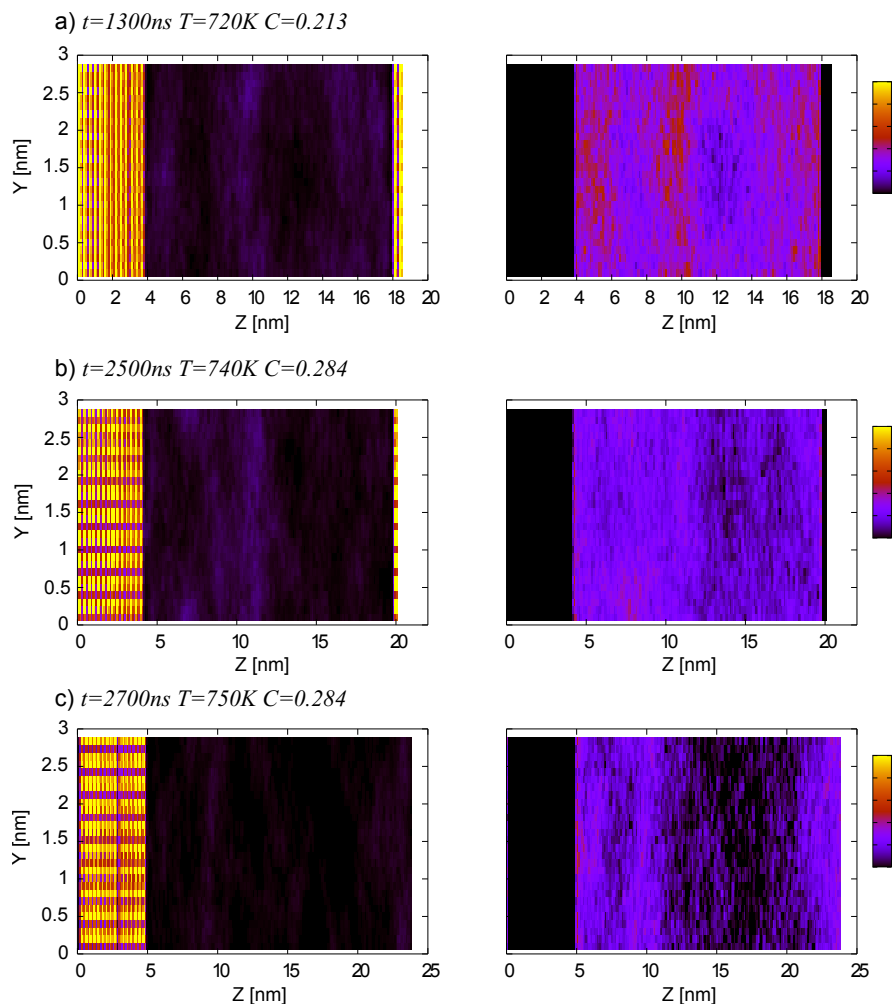


Fig. 9 Number density maps at 450bar. Left and right figures show the number densities of ions and water, respectively.

high density liquid phase could carry ions enough long time. Otherwise, rapid crystallization occurred. As a result, the porous morphology of the crystal was observed. Our simulation also suggested that there was the liquid-vapor coexistence phase during the flush crystallization under high pressure and the porous morphology could be found under low pressure owing to rapid crystallization.

4 Conclusion

We have conducted molecular dynamics simulations at three different pressures (i.e. 150bar, 250bar, and 450bar). They were under the critical pressure of water, between the critical pressure of pure water and the critical pressure of the vapor-

solid region of the sodium chloride solution, and above the critical pressure of the vapor-solid region, respectively. By using correlation between the number density of ions and water, solution state was parameterized well. It enables us to evaluate whether there is two phase fluid in the system or not. The correlation was dramatically different among those three pressures. It is interpreted with the combination of number density map that two phase vapor-liquid fluid became stable following the phase diagram as the pressure increased. At the lowest pressure, 150bar, the isolated crystal, which may construct porous geometry, was observed because crystallization was significantly fast. The fact agrees with the experimental observation and it also supports the proposed mechanism of crystal morphology difference at different pressures.

Acknowledgements The authors acknowledge the financial support of the Japanese Society for the Promotion of Science (JSPS) through a Grant-in-Aid for Scientific Research A (no. 24246148), JOGMEC, JST/JICA-SATREPS, and JAPEX. We also wish to thank Yasuhiro Fukunaka for valuable discussions.

References

1. Armellini, F. J., Tester, J. W.: Experimental Methods for Studying Salt Nucleation and Growth from Supercritical Water. *J. Supercritical Fluids* 4, 254-264 (1991)
2. Armellini, F. J., Tester, J. W., Hong, G. T.: Precipitation of Sodium Chloride and Sodium Sulfate In Water from Sub- to Supercritical Conditions: 150 to 550 °C, 100 to 300 bar. *J. Supercritical Fluids* 7, 147-158 (1994)
3. Hovland, M., Kuznetsova, T., Rueslatten, H., Kvamme, B., Johnsen, H. K., Fladmark, G. E., Hebach, A.: Sub-surface precipitation of salts in supercritical seawater. *Basin Research* 18, 221-230 (2006)
4. Butterfield, D. A., McDuff, R. E., Mottl, M. J., Lilley, M. D., Lupton, J.E., Massoth, G. J.: Gradients in the composition of hydrothermal fluids from the Endeavour segment vent field; Phase separation and brine loss. *J. Geophysical Research*, 99, 9561-9583 (1994)
5. Koschinsky, A., Garbe-Schonberg, D., Sander, S., Schmidt, K., Gennerich, H., Stauss, H.: Hydrothermal venting at pressure-temperature conditions above the critical point of seawater, 5°S on the Mid-Atlantic Ridge. *Geology* 36, 615-618 (2008)
6. Kitazono, S., Ueno, H.: Mineralogical and Genetical Aspects of the Doyashiki Kuroko Deposits, Hokuroku Basin. *Japan, Resource Geology* 53, 143-153 (2003)
7. Massoth, G. J., Butterfield, D. A., Lupton, J. E., McDuff, R. E., Lilley, M. D., Jonasson, I. R.: Submarine venting of phase-separated hydrothermal fluids at Axial Volcano, Juan de Fuca Ridge. *Nature* 340, 702-705 (1989)
8. Von Damm, K. L.: Chemistry of hydrothermal vent fluids from 9°-10°N, East Pacific Rise: "Time zero," the immediate post-eruptive period. *J. Geophysical Research* 105, 11203-11222 (2000)
9. Butterfield, D. A., Massoth, G. J., McDuff, R. E., Lupton, J. E., Lilley M.: Geochemistry of Hydrothermal Fluids From Axial Seamount Hydrothermal Emissions Study Vent Field, Juan de Fuca Ridge: Subseafloor Boiling and Subsequent Fluid-Rock Interaction. *J. Geophysical Research* 95, 12895-12921 (1990)
10. Haymon, R. M., Fornari, D. J., Von Damm, K. L., Lilley, M. D., Perfit, M. R., Edmond, J. M., Shanks, III W. C., Lutz, R. A., Grebmeier, J. M., Carbotte, S., Wright, D., McLaughlin, E., Smith, M., Beedle, N., Olson, E.: Volcanic eruption of the mid-ocean ridge along the East Pacific Rise crest at 9°45-52'N: Direct submersible observations of seafloor phenomena associated with an eruption event in April, 1991. *Earth and Planetary Science Lett.* 119, 85-101 (1993)
11. Moss, R., Scott, S. D.: Geochemistry and Mineralogy of Gold-Rich Hydrothermal Precipitates from The Eastern Manus Basin, Papua New Guinea. *The Canadian Mineralogist* 39, 957-978 (2001)

12. Hannington, M., Herzig, P., Stoffers, P., Scholten, J., Botz, R., Garbe-Schonberg, D., Jonasson, I. R., Roest, W.: Shipboard Scientific Party, First Observations of high-temperature submarine hydrothermal vents and massive anhydrite deposits off the north coast of Iceland. *Marine Geology* 177, 199-220 (2001)
13. Hirschmann, M., Kohlstedt, D.: Water in Earth's mantle. *Phys. Today* 65, 40 (2012)
14. Bermejo, M. D., Cocero, M. J.: Supercritical Water Oxidation: A technical Review. *AIChE J.* 52, 3933-3951 (2006)
15. Hess, B., Kutzner, C., van der Spoel, D., Lindahl, E.: GROMACS 4: Algorithms for Highly Efficient, Load-Balanced and Scalable Molecular Simulation. *J. Chem. Theory Comput.* 4, 435 (2008)
16. Berendsen, H. J. C., Grigera, J., Staatsma, T.: The missing term in effective pair potentials. *J. Phys. Chem.* 91, 6269 (1987)
17. Alejandre, J., Tildesley, D., Chapela, G.: Molecular dynamics simulation of the orthobaric densities and surface tension of water. *J. Chem. Phys.* 102, 4574 (1995)
18. Joung, I. S., Cheatham III, T. E.: Determination of alkali and halide monovalent ion parameters for use in explicitly solvated bio molecular simulations. *J. Phys. Chem. B* 112, 9020 (2008)
19. Joung, I. S., Cheatham III, T. E.: Molecular dynamics simulations of the dynamic and energetic properties of alkali and halide ions using water-model-specific ion parameters. *J. Phys. Chem. B* 113, 13279 (2009)
20. Bischoff, J. L., Pitzer, K. S.: Liquid-Vapor Relations for The System NaCl-H₂O: Summary of The P-T-x Surface from 300° to 500°C. *American Journal of Science* 289, 217-248 (1989)
21. Pitzer, K. S.: Aqueous Electrolytes at Near-Critical and Supercritical Temperatures. *International Journal of Thermophysics* 19, 355-365 (1998)
22. Driesner, T., Heinrich, C. A.: The system H₂O-NaCl. Part I: Correlation formulae for phase relations in temperature-pressure-composition space from 0 to 1000°C, 0 to 5000bar and 0 to 1 X_{NaCl}. *Geochimica et Cosmochimica Acta* 71, 4880-4901 (2007)
23. Walther, J. V.: *Essential of Geochemistry*, pp.137. Jones and Bartlett Publishers, Massachusetts (2009)
24. Nose, S.: A molecular dynamics method for simulations in the canonical ensemble. *Mol. Phys.* 52, 255 (1984)
25. Parrinello, M., Rahman, A.: Polymorphic transitions in single crystals: A new molecular dynamics method. *J. Chem. Phys.* 76, 2662 (1982)
26. Humphrey, W., Dalke, A., Schulten, K.: VMD: Visual molecular dynamics. *J. Mol. Graphics* 14, 33-38 (1996)